https://doi.org/10.30799/jespr.220.22080201 J. Environ. Sci. Pollut. Res. - Volume 8 Issue 2 (2022) 471–474

Share Your Innovations through JACS Directory

Journal of Environmental Science and Pollution Research

Visit Journal at https://www.jacsdirectory.com/jespr

ISSN: 2455-0272

Carica papaya Leaves Extract for Biosynthesis of Nanoparticles and Their Application

C.K. Potdar, H. Jain, R.B. Dixit*

Ashok and Rita Patel Institute of Integrated Study and Research in Biotechnology and Allied Sciences (ARIBAS), Affiliated to CVM University, New Vallabh Vidyanagar – 388 121, Gujarat, India.

ARTICLEDETAILS

Article history:
Received 29 May 2022
Accepted 18 June 2022
Available online 24 July 2022

Keywords:
Silver Nanoparticles
Methylene Blue Dye
Carica papaya

ABSTRACT

In the last few decades' surface water, under river flow, groundwater and frozen water shows the presence of pollutant due to dyes containing chemicals waste from dyes and textile related Industries. One of the such methylene blue dye is utilized for coloring paper, temporary hair coloring, dyeing of cotton and wools, as a result its effluents is contaminated with methylene blue dye. Removal of the dyes from the effluent is of very important due to the serious environmental hazards that can result into sever health damages, particularly for human being. Therefore, there is a need to resolve the implications caused by dye pollution. Recently nanoparticles are reported for the dye removal from the industrial waste water. Therefore, effluent treatment using nanosize particles as an adsorbent provides more surface area, less time consumption, eco-friendly, easy and cost-effective process. In the present study, efforts were made to study the potential of silver nanoparticles for the removal of methylene blue dyes from aqueous solution was greatly explored. For this purpose, silver nanoparticles were synthesized using Carica papaya methanolic leaves extract and were characterized by spectral techniques. The adsorption study was conducted by batch equilibrium method. To achieve the optimum adsorption conditions, the influence of initial dye concentration and contact time on the removal efficiency of dye has been studied.

1. Introduction

In nearby industrial area, the quality of water resources is degraded due to the release of toxic effluents from surrounding industries. It is found that around 20% of the total textile dyes output is being discharged into the environment as an effluent. Most of the azo dyes are toxic chemicals that are entering in human bodies through water, air, soil, animals and plants. It can cause cancer, skin irritation, and respiratory diseases [1]. Methyleneblue (MB) dye is being used for colouring the textile materials, fabrics, paper, silk and microscopy stain, medical agents, and in cosmetic dyeing [2]. It is a high-consumption dye pigment, was considered as a model organic pollutant, and its degradation was investigated in the presence of magnetite (Fe_3O_4) under UV and solar illumination [2]. Chemically, methylene blue dye is a cationic thiazine moiety (tetramethylthionine chloride) and can cause the most severe diseases and therefore, it's essential to identify an effective catalyst for removing this hazardous dye and treating methylene blue - contaminated wastewater [3]. Till date various processes are widely used for the dye removal from the industrial waste. However, the majority of them is prohibitively expensive, inaccessible, and are not suitable in some circumstances [3]. Now a day nanotechnology offered new opportunities for developing pioneering methods to treat dye-contaminated wastewater [4,5]. Nano-size silver nanoparticles having unique electron conduction properties and surface properties. Majority of synthetic approaches for preparing nano size silver particles involve the use of harmful chemicals as reducing agents as well as use of polymers, dendrimers and surfactants, as capping agents, or simply harsh reaction conditions that may generate toxic side products, resulting in pollution [2]. Because of the detrimental effects of the above-mentioned synthetic processes, new synthetic approaches have been developed, which utilize biological resources to produce nanoparticles [2]. Bioagents such as plants and microbes such as algae, bacteria and fungi are used in the green synthesis of metallic nanoparticles [6]. Biologically derived nanoparticles are an eco-friendly, low-cost, energy-efficient, and are easy-to-scale-up. Polyphenolic compounds, amino acids, proteins, vitamins and terpenoids are significant stabilizing and reducing agents in the green production of silver nanoparticles [6,7].

Looking to above advantages of green synthesis of silver nanoparticles, we report here the synthesis of silver nanoparticles using bioactive compound obtained from *Carica papaya* leaves extract. Resultant extract is effective for the removal of methylene blue dye from the aqueous solution. Batch equilibrium method was used to determine the efficiency of adsorption of methylene blue dye using zero valent silver (Ag^0) nanoparticles (AgNPs). The key parameters such as pH, contact time, initial dye concentration and adsorbent dose were considered in the present study.

2. Experimental Methods

2.1 Material

All the reagents were prepared in double distilled water. Precursors used were of analytical grade. Fresh leaves of *Carica papaya* plant were collected from nearby farm of Gana, Anand, Gujarat, India.

2.2 Methods

To prepare *Carica papaya* leaves extract, fresh leaves were rinsed multiple times using double distilled water and then dried in sun light for few days. To create a homogeneous fine powder, the dried leaves were milled in a mixer grinder and sieved through 60# size filters. Homogeneous powder of *Carica papaya* leaves (20 grams) was mixed well with distilled water and agitated at 80 °C for 30 to 40 minutes. The resultant mixture after cooling down at room temperature was filtered using Whatman filter paper (No 1). The filtrate was dark in color and was stored at 4 °C for further use [1, 8] and it was used as a reducing agent for the preparation of silver nanoparticles.

2.3 Preparation of AgNPs

Synthesis of silver (Ag^0) nanoparticles was carried out using silver nitrate. For that 5 mL of *Carica papaya* leaves extract and 30 mL of 1 milimolar silver nitrate solution were taken in a 250 mL conical flask and stirrer well for 1 hr at 70 °C. After 40 minutes color of solution was changed to dark brown. The change in color of the solution indicates the

*Corresponding Author:ritsdixit@yahoo.co.in(R. Dixit)

https://doi.org/10.30799/jespr.220.22080201

formation of nanoparticles. The resultant mixture was further stirred for 20 minutes, resulting in to intense brown colored solution indicating the formation of silver nanoparticles. The obtained brown colored solution was centrifuged at 10000 rpm and particles obtained were washed 2 to 3 times with ethanol, dried and stored in sealed air tight tube [8].

2.4 Characterization

To measure the absorbance of silver nanoparticles a Systronics Spectrophotometer 104 was used. Absorbance spectra were recorded in the wavelength range of 350 – 600 nm with a resolution of 1 nm in a quartz cuvette having 1 cm path length. To determine the presence of biomolecules on the surface of the AgNPs nanoparticles, using FT-IR spectrophotometer Perkin Elmer spectrum GX, FTIR study was carried. The spectra of the sample were carried out in a KBr pellets in the range of 8000 – 400 cm^{-1}. To perform X-ray diffraction analysis of the silver nanoparticles, D8 Advance X-ray diffractometer (Brucker, Dresden, Germany) with CuKα1 radiation was used. The measured diffraction pattern was compared with standard values to account for the crystalline structure of AgNPs.

2.5 Preparation of Methylene Blue Dye Stock Solution and Standard Solution

A stock solution of 1000 ppm methylene blue dye was prepared by dissolving 0.1 g of it in 100 mL double distilled water. Standard solution was prepared by diluting stock solution in appropriate concentration.

2.6 Dye Removal Experiments

For dye removal experiments batch equilibrium method was used. For this purpose, a series of methylene blue dye solution with varied concentration were prepared. Accordingly, 25 mL of methylene blue dye solution was taken in a beaker along with 0.1 g of AgNPs. The solutions containing beakers were kept in mechanical shaker at the agitation speed of 300 revolutions per minute. The study of effect of time on the adsorption phenomena on AgNPs was carried out in a time interval of 10 - 15 minutes. The effect of pH on methylene blue dye adsorption on AgNPs was carried out at room temperature in a 2.30 hrs. The pH values were adjusted in the range of 2 – 10 using 0.1 M HCl or 0.1 M NaOH solution. The effect of adsorbent dose on methylene blue dye adsorption was carried out with 10 mg to 40 mg of AgNPs dosage. Using spectrophotometer, concentration of methylene blue dye was estimated and the % of removal of methylene blue dye from aqueous solution was estimated using the following formula (1):

$$\% \, Removal = Co - \frac{Ce}{Co} \times 100 \qquad (1)$$

Where, C_o is the initial concentration of methylene blue dye (mgL^{-1}) and C_e is the final concentration of methylene blue dye (mgL^{-1})

2.7 Evaluation of Adsorption Performance

For analyzing sorption equilibrium parameter, the adsorption isotherm is essential for explaining the mechanism of solutes interaction with the adsorbent. In this study the percentage removal of methylene blue dye from aqueous solution was estimated using Langmuir (Eq. (2)) and Freundlich (Eq. (3)) isotherms models. It was prepared using a straight-line equation, and all the parameters for the methylene blue dye adsorption were determined. Following equations were used for the Langmuir (2) and Freundlich (3) models.

$$\frac{1}{qe} = \frac{1}{Kl*qm} * \frac{1}{ce} + \frac{1}{qm} \qquad (2)$$

Where, qe is the dye adsorbed per unit mass, Ce is the adsorbate concentration, qm is the maximum adsorption capacity, Kl is the Langmuir constant.

$$\text{Log}\, qe = \log Kf + \frac{1}{n} \log ce \qquad (3)$$

where K_f is the freundlich constant, n is the heterogenicity factor, qe is the adsorption capacity.

3. Results and Discussion

3.1 Characterization

The synthesized AgNPs were detected visually and by Ultraviolet–visible spectrophotometry. Nanoparticles were strongly absorbed in the Ultraviolet–visible region [9], due to interaction between incident radiations and electrons on the surface of nanoparticles. Optimizing parameters during synthesis of nanoparticles is a critical step in obtaining the correct size and shape of AgNPs. When aqueous extracts of *Carica papaya* leaves were treated with 1 mM aqueous solution of silver nitrate solution, the reduction of pure Ag^+ ions to Ag° takes place and it was observed by monitoring the reaction media using UV-Vis spectra. For this purpose, 0.50 mL of AgNPs solution was taken in cuvette and was diluted by adding 2.5 mL of distilled water. Colloidal silver [11] exhibits a characteristic absorption band at 412.87 nm and at 0.033 Abs.

FTIR spectrum of *Carica papaya* leaves extract and synthesized AgNPs are shown in Fig. 1. The major absorption bands in *Carica papaya* leaves extract were observed at 3422.55 cm^{-1}, 2921 cm^{-1} and 1631.08 cm^{-1} attributed to O–H stretching [9] confirms the presences of the phenolic O–H group, two weak bands at 1631 cm^{-1} and 1383.99 cm^{-1} associated with N–H bending and C=O stretching vibrations respectively, while a peak at 1154.22 cm^{-1} is observed due to C-N stretching vibrations. The synthesized AgNPs nanoparticles [12] showed a band at 3427.55, 2921.27, 1631.25 and 1317.62 cm^{-1}. Comparison of IR spectrum of *Carica papaya* leaves extract with biosynthesized silver nanoparticles indicates the presences of similar bands in both the spectrum with small change in intensity and absorption. A band at 1317.62 cm^{-1} in AgNPs attributed to NO_3^{-1} suggested that aggregation of AgNPs is protected by nitrate ions.

The FTIR spectra of dye bound nanoparticles (Fig. 2) were carried to confirm adsorption of dye on nanoparticles. All the peaks present in nanoparticles were retained except the one at 1382 cm^{-1} which shifted and reduced transmittance due to adsorbed dye. The peak corresponds to C=O which might be lost due to weak bond formation between dye and nanoparticles.

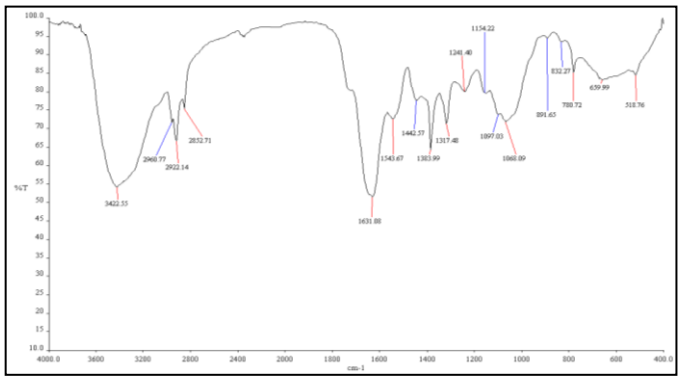

Fig. 1 FTIR spectrum of synthesized AgNPs

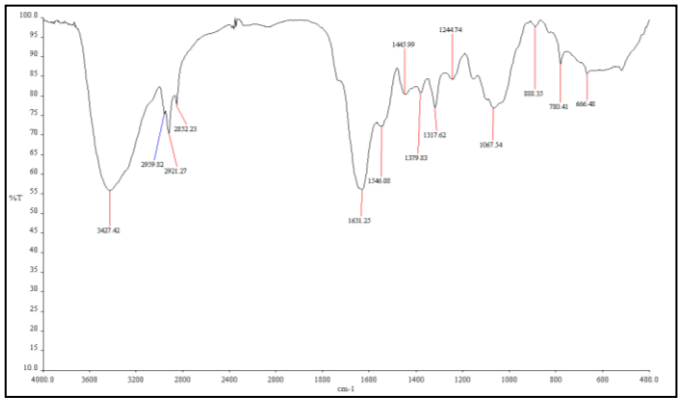

Fig. 2 FTIR spectrum for dye bound nanoparticles (AgNPs)

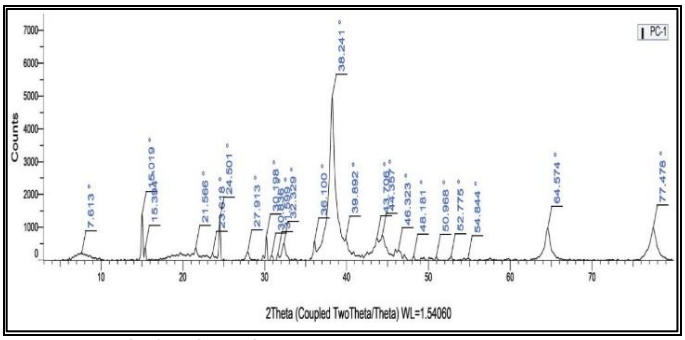

Fig. 3 XRD graph of synthesized AgNPs

https://doi.org/10.30799/jespr.220.22080201

X-ray diffraction is used to define the particle size and crystallinity of synthesized silver nanoparticles and is shown in Fig. 3. In XRD graph, 2θ values is appeared at the angles of 38.2°, 44.3°, 64.5° and 77.4° respectively correspond to diffraction indexed to (1 1 1), (2 0 0), (2 2 0) and (3 1 1) respectively. Obtained values suggests that the highest intensity of peak is observed at 38.20° for 111 indicates that synthesized nanoparticles are abundantly distributed in 111 plane and are polycrystalline Face-Cantered Cubic (FCC). Further, the average particle size was calculated as 27.99 nm using Scherrer's equation [13], $D = 0.9\lambda/\beta\cos\theta$, where, D is the crystallite size, θ is the Bragg angle, β is the width at half maximum, λ is the wavelength of X-ray.

3.2 Batch Adsorption Experiment

Dye adsorption experiment was conducted in batch mode using 50 mL stock solution of synthesized AgNPs and methylene blue dye solution and was stirred well by magnetic stirrer for 30 minutes. Finally, the solution was filtered by vacuum filtration and was analyzed by UV-Visible spectrophotometer at 500 nm wavelength. Concentration of the dye solution was determined using absorbance value of solution before and after contact with the adsorbent dose. The studies performed were of contact time, initial dye concentration, pH, temperature and adsorbent dose [14-18].

3.3 Effect of Contact Time on Percentage Dye Removal

It was tested using a 10-ppm initial dye concentration and a 40 mg adsorbent. Fig. 4 shows that initial uptake of dye was faster, resulting in a highest elimination of 84.6% after 60 minutes of attaining equilibrium. The dye absorption was initially greater, but subsequently it began to slow down, possibly due to shortage of active available surface area for dye absorption. The comparative increase in dye removal after 60 minutes of contact time was not significant [19].

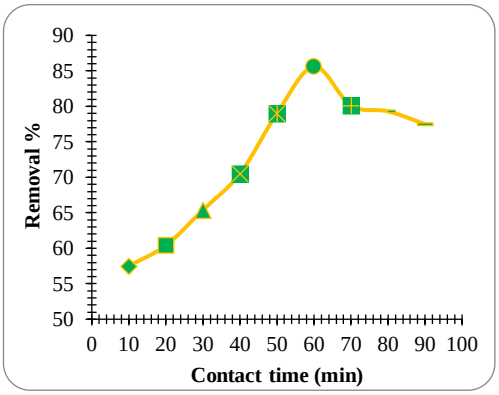

Fig. 4 Effect of contact time on the methylene blue dye uptake

3.4 Effect of Adsorbent Dosage on Percentage Dye Removal

This section illustrates the effect of adsorbent dose on percentage dye removal since a trade-off between the adsorbent dose and % methylene blue dye elimination is significant. Fig. 5 shows that as adsorbent concentrations rise from 10 to 60 mg, the highest 84% removal occurs at 40 mg dose of MB dyes. The %adsorption rises with rise in AgNPs and then starts to decrease with increase in amount of AgNPs. This could be due to the fact that as the AgNPs dosage increases, surface area and the number of available adsorption sites increases, resulting in increased in the dye adsorption. As equilibrium is reached, adsorption decreases [20].

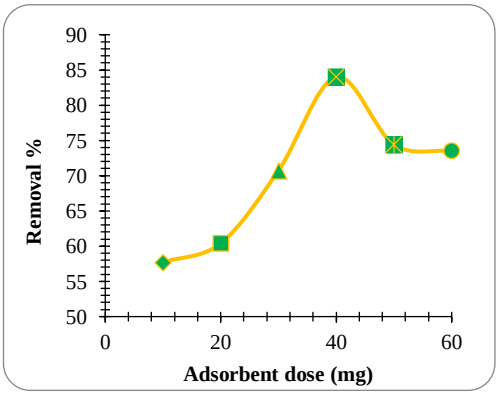

Fig. 5 Effect of adsorbent dose on the MB dye uptake

3.5 Effect of pH on Methylene Blue Dye Uptake

The pH is a critical parameter that affects the capacity of any adsorbent to remove MB dye among the all-other parameters that affect dye removal. Fig. 6 shows the relationship between the pH of the solution and the percentage removal of methylene blue dye. The pH in this study varied from acidic pH to alkaline pH. Maximum adsorption was studied with an initial dye concentration of 10 ppm using 40 mg of AgNPs. The solution mixture was shaken for 2 hours at 120 rpm on a mechanical shaker. At basic pH 8, the greatest adsorption (79.9 %) was observed (Fig. 6). The sulfonic group present in MB dyes dissociates in aqueous solution and was converted to anionic dye ions. The surface of nanoparticles is neutral, when it is added to the dye solution it donates an electron to methylene blue dye and forms a cation. MB dyes accepts the electron and gets reduced to leucomethyl blue which is a colourless compound. The reducing agent present in extract gives an electron to Ag cation formed and brings it back to stable Ag. This electron relay mechanism is observed in dye removal [11].

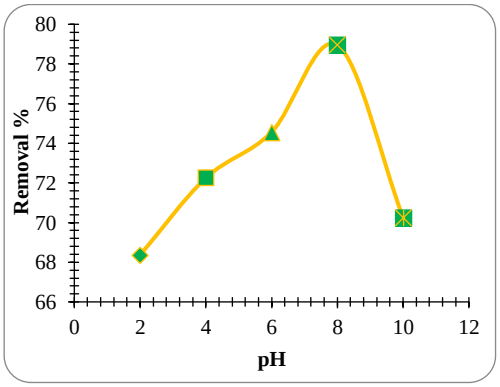

Fig. 6 Effect of pH on the methylene blue dye uptake

3.6 Effect of Initial Dye Concentration on Methylene Blue Dye Uptake

The effect of the initial MB dye concentration on the rate of absorption of MB dye on synthesized AgNPs was studied. As the initial MB dye concentration increased, the adsorption on AgNPs percentage decreased. As the dye concentration rise from 2 ppm to 10 ppm, the adsorption capability of AgNPs increased from 35 to 75.32 % and is shown in Fig. 7. Upon addition of AgNPs to the MB dye solution equilibrium was reached after 60 minutes of maximum dye sequestration. It shows that MB dye uptake increased as concentration of AgNPs increased until equilibrium was reached, at which point there was no further dye uptake due to the lack of void space for dye absorption [20].

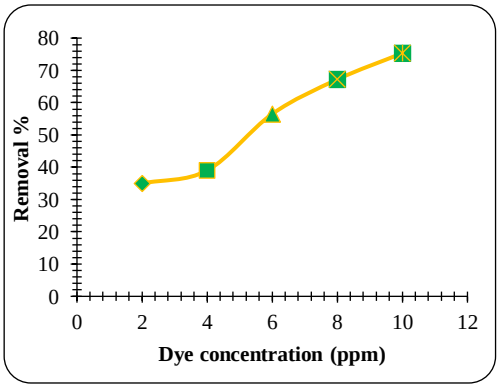

Fig. 7 Effect of MB dye concentration on the dye uptake

3.7 Adsorption Equilibrium Isotherm

Adsorption equilibrium isotherms show how the initial concentration affects the adsorption quantity. To estimate the adsorption isotherm for methylene blue dye removal using AgNPs synthesised silver nanoparticles, a known models were used, and the data are reported in Table 1.

3.8 Langmuir Equilibrium Isotherm

Langmuir model is used to describe the monolayer adsorption of a MB dye from a solution on the surface of AgNPs having a large number of similar sites. This model assumes homogeneous adsorption rates onto the surface of synthesized silver nanoparticles. As a result, this model was primarily adopted for estimating the maximal adsorption capacity, which

https://doi.org/10.30799/jespr.220.22080201

simply corresponds to the adsorbent's monolayer surface. Langmuir isotherm equation is shown as below:

$$\frac{1}{qe} = \frac{1}{Kl \text{ x } qm} \text{ x } \frac{1}{ce} + \frac{1}{qm}$$

To calculate qm and Kl, the slope and intercept were obtained by plotting the Langmuir isotherm graph (Fig. 8). A dimensionless constant separation factor can be used to express the Langmuir isotherm (RL). The term "RL" can be defined as:

$$RL = \frac{1}{1 + (Kl \text{ x } Ce)}$$

The RL values reflect the isotherm type; if RL > 1, the isotherm is unfavourable; if RL = 1, the isotherm is favourable and if RL = 0, the isotherm is irreversible. The current results (RL value) 0.027 indicating that adsorption was favourable [19–21].

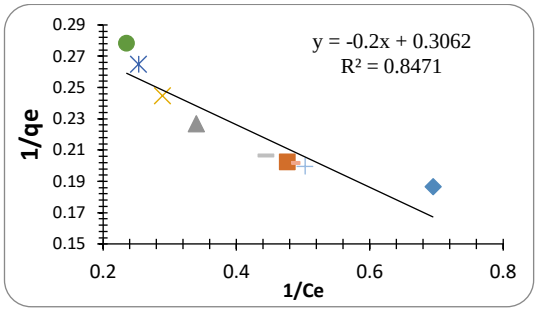

Fig. 8 Langmuir isotherm for synthesized AgNPs

3.9 Freundlich Isotherm

The Freundlich isotherm model, can be used to illustrate the "relationship between non-ideal and reversible adsorption" on a heterogeneous surface. The linear equation is given bellow:

$$\text{Log } qe = \log kf + \frac{1}{n} \log ce$$

where, 'n' and 'K_f' are Freundlich constants.

The values for K_f and 'n' can be determined by drawing the graph between log qe and log Ce (Fig. 9) and are reported in Table 1. The data showed that this adsorption fits the Langmuir isotherm model better than the Freundlich isotherm model [19-21].

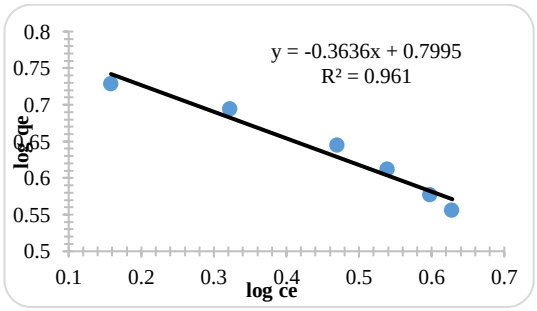

Fig. 9 Freundlich isotherm for synthesized AgNPs

Table 1 Langmuir and Freundlich isotherm study for synthesized AgNPs

Isotherm linear equation	Langmuir			Freundlich		
Parameters	R^2	Kl	q_{max}	Kf	N	R^2
Obtained value	0.980	3.56	17.30	0.808	5.373	0.999

4. Conclusion

Using *carica papaya* leaves extract silver nanoparticles were successfully synthesized via green synthesis method. The synthesized silver nanoparticles appeared dark brown in color. To confirm the synthesis of nanoparticles various analytical technique such as UV- Visible spectroscopy, FTIR, XRD were performed. UV-Visible peak was observed at 412 nm which gave preliminary confirmation of synthesized nanoparticles. The different functional group present on nanoparticles was identified using FTIR spectra. The particle size and crystalline structure were predicted by XRD. The shape of nanoparticles was face centered cubic (fcc) and average particle size was 27 nm, this characterization results confirmed the synthesis of nanoparticles. Batch adsorption study was used to optimize various parameters responsible for adsorption of methylene blue dye from aqueous solution. Various parameters were optimized as 60 min, 8 pH, 40 mg and 10 ppm respectively. Maximum dye removal efficiency was observed as 84% at optimized conditions. The mechanism of adsorption of dye on nanoparticles was confirmed by plotting adsorption isotherms. In this study type of adsorption mechanism were confirmed via Langmuir and Freundlich adsorption isotherm study. The isotherm data reveals binding of dye on nanoparticles surface as both monolayer and multilayer.

Acknowledgements

Authors are gratefully acknowledged to Charutar Vidya Mandal and CVM University, Vallabh Vidyanagar and Head, ARIBAS for providing research facility. The service of Director, SICART, Vallabh Vidyanagar, for spectral analysis is gratefully acknowledged.

References

[1] M.S.H. Bhuiyan, M.Y. Miah, S.C. Paul, A.T. Das, O. Saha, et al., Green synthesis of iron oxide nanoparticle using *Carica papaya* leaf extract: application for photocatalytic degradation of remazol yellow RR dye and antibacterial activity, Heliyon 6(8) (2020) e04603 (1-13).
[2] K.M. Reza, A. Kurny, F. Gulshan, Photocatalytic Degradation of methylene blue by magnetite + H_2O_2 + UV Process, Int. J. Environ. Sci. Develo. 7(5) (2016) 325–329.
[3] L. David, B. Moldovan, Green synthesis of biogenic silver nanoparticles for efficient catalytic removal of harmful organic dyes, Nanomater. 10(2) (2020) 202 (1-16).
[4] R.D. Saini, Textile Organic Dyes: Polluting effects and elimination methods from textile waste water, Int. J. Chem. Eng. Res. 9(1) (2017) 121–136.
[5] I. Khan, K. Saeed, I. Khan, Nanoparticles: Properties, applications and toxicities, Arabian J. Chem. 12(7) (2019) 908–931.
[6] M. Mahadevi, A.S. Madhavan, Natural movement and therapeutic different bioactive constituents and biochemical composition of (*Carica papaya* L.), Int. J. Bot. Studies. 6(5) (2021) 224-228.
[7] M. Darroudi, M.B. Ahmad, A.H. Abdullah, N.A. Ibrahim, Green synthesis and characterization of gelatin-based and sugar-reduced silver nanoparticles, Int. J. Nanomed. 6(1) (2011) 569–574.
[8] M.M. Goudarzi, M. Mousavi-Kamazani, S. Bagheri, M. Salavati-Niasari, Biosynthesis and characterization of silver nanoparticles prepared from two novel natural precursors by facile thermal decomposition methods, Sci. Reports 6 (2016) 1–13.
[9] T. N. J. I. Edison, R. Atchudan, R.C. Kamal, Y. R. Lee, *Caulerpa racemosa*: a marine green alga for eco-friendly synthesis of silver nanoparticles and its catalytic degradation of methylene blue, Biopro. Biosyst. Eng. 39(9) (2016) 1401–1408.
[10] S.P. Singh, A. Mishra, R.K. Shyanti, R.P. Singh, A. Acharya, Silver nanoparticles synthesized using *Carica papaya* leaf extract (AgNPs-PLE) causes cell cycle arrest and apoptosis in human prostate (DU145) cancer cells, Bio. Trace Elem. Res. 199(4) (2021) 1316–1331.
[11] M. Vanaja, K. Paulkumar, M. Baburaja, S. Rajeshkumar, G. Gnanajobitha, et al., Degradation of methylene blue using biologically synthesized silver nanoparticles, Bioinorg. Chem. Appl. 2014 (2014) 7423 (1-8).
[12] K. Khan, S. Javed, Silver nanoparticles synthesized using leaf extract of Azadirachta indica exhibit enhanced antimicrobial efficacy than the chemically synthesized nanoparticles: A comparative study, Sci. Prog. 104(2) (2021) 1–15.
[13] T. Sinha, M. Ahmaruzzaman, Green synthesis of copper nanoparticles for the efficient removal (degradation) of dye from aqueous phase, Env. Sci. Pol. Res. 22(24) (2015) 20092–20100.
[14] S.D. Alexandratos, A.W. Trochimczuk, E.P. Horwitz, R.C. Gatrone, Synthesis and characterization of a bifunctional ion exchange resin with polystyrene-immobilized diphosphonic acid ligands, J. Appl. Polym. Sci. 61(2) (1996) 273-278.
[15] K. Singh, D.H. Lataye, K.L. Wasewar, Removal of fluoride from aqueous solution by using low-cost sugarcane bagasse: kinetic study and equilibrium isotherm analyses, J. Hazard. Toxic Radioact. Waste 20(3) (2016) 1-6.
[16] M.B. Desta, Batch sorption experiments: Langmuir and Freundlich isotherm studies for the adsorption of textile metal ions onto Teff Straw (*Eragrostis teff*) agricultural waste, J. Thermo. 2013(1) (2013) 1-6.
[17] R.S. Lokhande, P.U. Singare, D.S. Pimple, Study on physico-chemical parameters of waste water effluents from Taloja industrial area of Mumbai, India, Int. J. Ecosystem. 1(1) (2011) 1-9.
[18] X. Zhao, L. Baharinikoo, M.D. Farahani, B. Mahdizadeh, A.A.K. Farizhandi, Experimental modelling studies on the removal of dyes and heavy metal ions using $ZnFe_2O_4$ nanoparticles, Sci. Rep. Nature Portfolio 12(5987) (2022) 1-15.
[19] S. Saruchi, P. Thakur, V. Kumar, Kinetics and thermodynamic studies for removal of methylene blue dye by biosynthesize copper oxide nanoparticles and its antibacterial activity, J. Env. Health Sci. Eng. 17(1) (2019) 367–376.
[20] M.H. Ehrampoush, M. Miria, M.H. Salmani, A.H. Mahvi, Cadmium removal from aqueous solution by green synthesis iron oxide nanoparticles with tangerine peel extract, J. Env. Health Sci. Eng. 13(84) (2015) 1–7.
[21] Y. Sharma, R. Bhateria, Phytoproduction of iron nanoparticles for methyl orange removal and its optimization studies, Plant Arch. 21(1) (2021) 939–954.

https://doi.org/10.30799/jespr.220.22080201

Cite this Article as: C.K. Potdar, H. Jain, R.B. Dixit, *Carica papaya* leaves extract for biosynthesis of nanoparticles and their application, J. Env. Sci. Pollut. Res. 8(2) (2022) 471–474.